Design of a scanning laser meter for monitoring the spatio-temporal evolution of snow depth and its application in the Alps and in Antarctica

Ghislain Picard, Laurent Arnaud, Jean-Michel Panel, Samuel Morin

The Cryosphere, 10, 1495–1511, 2016
www.the-cryosphere.net/10/1495/2016/
doi:10.5194/tc-10-1495-2016

The Cryosphere Open Access EGU

Design of a scanning laser meter for monitoring the spatio-temporal evolution of snow depth and its application in the Alps and in Antarctica

Ghislain Picard[1,2], Laurent Arnaud[1], Jean-Michel Panel[3], and Samuel Morin[3]

[1]UGA/CNRS, Laboratoire de Glaciologie et Géophysique de l'Environnement (LGGE) UMR 5183, Grenoble, 38041, France
[2]ACE CRC, University of Tasmania, Private Bag 80, Hobart, TAS 7001, Australia
[3]Météo-France – CNRS, CNRM UMR 3589, Centre d'Études de la Neige, Grenoble, France

Correspondence to: Ghislain Picard (ghislain.picard@ujf-grenoble.fr)

Received: 14 March 2016 – Published in The Cryosphere Discuss.: 30 March 2016
Revised: 2 June 2016 – Accepted: 17 June 2016 – Published: 18 July 2016

Abstract. Although both the temporal and spatial variations of the snow depth are usually of interest for numerous applications, available measurement techniques are either space-oriented (e.g. terrestrial laser scans) or time-oriented (e.g. ultrasonic ranging probe). Because of snow heterogeneity, measuring depth in a single point is insufficient to provide accurate and representative estimates. We present a cost-effective automatic instrument to acquire spatio-temporal variations of snow depth. The device comprises a laser meter mounted on a 2-axis stage and can scan $\approx 200\,000$ points over an area of 100–200 m^2 in 4 h. Two instruments, installed in Antarctica (Dome C) and the French Alps (Col de Porte), have been operating continuously and unattended over 2015 with a success rate of 65 and 90 % respectively. The precision of single point measurements and long-term stability were evaluated to be about 1 cm and the accuracy to be 5 cm or better. The spatial variability in the scanned area reached 7–10 cm (root mean square) at both sites, which means that the number of measurements is sufficient to average out the spatial variability and yield precise mean snow depth. With such high precision, it was possible for the first time at Dome C to (1) observe a 3-month period of regular and slow increase of snow depth without apparent link to snowfalls and (2) highlight that most of the annual accumulation stems from a single event although several snowfall and strong wind events were predicted by the ERA-Interim reanalysis. Finally the paper discusses the benefit of laser scanning compared to multiplying single-point sensors in the context of monitoring snow depth.

1 Introduction

Snow depth is one of the most important and basic characteristics of snow on the ground. Measurements and modelling of this variable is crucial for numerous applications, such as in hydrology (López-Moreno et al., 2013), avalanche forecasting (Schweizer, 2003), meteorology (de Rosnay et al., 2012) and for sea ice (Lecomte et al., 2011; Katlein et al., 2015) or permafrost research (Gisnås et al., 2016). Snow depth is commonly reported on in operational databases and measured at research monitoring stations or occasionally in the field. Many techniques are available to measure or monitor snow depth, the most common being manual measurements with a stick (e.g. Fierz et al., 2009) and ultrasonic ranging probes (Ryan et al., 2008). Their inherent accuracy is of the order of 1 cm which is largely sufficient for most applications. Nevertheless, the vast majority of these measurements are representative of a small area, typically less than 1 m^2, corresponding to the footprint of the sensor or the "homogeneous" area around the stick, whereas the spatial scale of interest is usually much larger than this, ranging from the area of meteorological monitoring stations (hundreds of square metres) to that of catchments (from a few square kilometres).

Since the snow cover is in general heterogeneous at any scales from the small scale to the application scale, the actual uncertainty of the snow depth in a given area is much larger than the inherent accuracy of individual measurements and is primarily governed by the spatial variability in this area (Neumann et al., 2006; Clark et al., 2011; Grünewald et al., 2013). This variability stems from a variety of processes. Snowfall repartition is not uniform (Scipión et al., 2013) because of the ground topography at metre-to-kilometre scales, vegetation and other obstacles. Wind transport tends to amplify heterogeneity because erosion and redeposition are sensitive to small initial differences in the snow properties. Sastrugi, dunes and other wind-formed features are frequent and their formations are still not well understood (Filhol and Sturm, 2015). Metamorphic and melt processes can also contribute to the decrease or increase of the spatial variations (Cathles et al., 2014). All these processes are complex and interact with each other so that the spatial variability can only be explicitly predicted using high-resolution atmospheric–snowpack coupled models (Mott et al., 2010; Vionnet et al., 2014). Simpler approximate approaches have been devised to implicitly represent and predict the variability (Clark et al., 2011; Libois et al., 2014). As a consequence, from the perspective of snow depth estimation with ground-based measurements, the spatial variability has to be considered random noise with largely unknown characteristics (Shook and Gray, 1996; López-Moreno et al., 2011; Trujillo and Lehning, 2015). In some extreme cases such as on the Antarctic Plateau, the mean annual accumulation (which is the snow depth change during a year) can even be smaller than the spatial standard variations of the distribution (Eisen et al., 2008; Libois et al., 2014). It means that in one point, net ablation or accumulation higher than twice the spatial average occurs frequently (Petit et al., 1982; Libois et al., 2014). In general, accurate snow depth estimate requires averaging many independent point measurements to reduce the impact of this noise. As minimizing the number of measurements is often of practical importance, a good knowledge of the spatial variability (i.e, the statistical properties of the noise) is required (Trujillo and Lehning, 2015).

Terrestrial laser scanning (TLS, Prokop, 2008; Deems et al., 2013) is a fast-developing tool for characterizing the spatial variability of snow depth. Recent advances have allowed improved range and increased density of measurements (number of points per square metre), thus allowing all the relevant scales from the metre scale to the application scale to be covered (Deems et al., 2013). Most studies have explored the rich spatial information content provided by TLS (e.g. Revuelto et al., 2014; Filhol and Sturm, 2015) but only used a few scans acquired at two or a few different dates (Deems et al., 2015). While this may be enough to estimate the seasonal peak accumulation or study snow redistribution processes and geomorphology of the surface (Revuelto et al., 2016), it is insufficient to capture the individual events that affect snow depth over a season. The cost of these devices – about 100 times the price of a single-ranging probe – and the constraints on the operating conditions make their deployment in the field for continuous monitoring relatively challenging. Nevertheless, this application is rapidly emerging (Hartzell et al., 2015) and it is expected that a few catchments will be instrumented in the coming years. A cheaper emerging alternative uses an unmanned autonomous vehicle with on-board camera and an image processing technique known as Surface from Motion (SfM, e.g. Jagt et al., 2015; Nolan et al., 2015) to construct digital elevation models from multiple images. A snow depth map is then derived by differentiating a no-snow acquisition taken before or after the snow season like with the TLS. While the technique can not reach vertical accuracy of 1 cm yet, the density of measurements and range are of the same order as those of modern TLS. Operating conditions also constrain, which limits the frequency as with TLS. The same approach can also be applied at a higher resolution (Nicholson et al., 2016) and seems promising for continuous monitoring.

The purpose of this paper is to introduce and evaluate the performances of a new instrument which, in terms of spatial range, acquisition frequency and cost, lies between the spatial-oriented techniques (TLS, SfM) and temporal-oriented techniques (ultrasonic and laser ranging probes). The initial aim of this development was to measure mean snow depth with accuracy approaching 1 cm at a temporal resolution adequate to capture precipitation and wind transport events, snow densification and melt. The instrument is able to scan areas of over a hundred square metres every day, for a cost less than 10 single ranging probes or at a tenth of the cost of a common TLS. The robustness is another important factor since our goal was to cover full snow seasons up to a year without attending the instrument in the harsh Antarctic conditions. As this factor was a strong constraint and drove many of our technical choices, the instrument is called the Rugged Laser Scan (RLS). Two instruments have been built: the first one has been deployed at the Col de Porte alpine site in the French Alps (45° N and 6° E, 1325 m altitude) (Morin et al., 2012) during one of the winter campaigns of the World Meteorological Organization-Snow Precipitation InterComparison Experiment (WMO-SPICE) project (winter season 2014–2015) with the specific aim of investigating the accuracy and value of the device compared to traditional ranging probes. The second has been set up at Dome C in Antarctica (75° S and 123° E) in December 2014 and has been operating most of the time for over 1 year until it was dismantled for maintenance and improvements. The specific objective was to observe the snow accumulation processes at daily-to-weekly temporal scales which are unaccessible with other glaciological methods, such as readings of stake emergence (Genthon et al., 2015).

The paper is organized as follows: Sect. 2 introduces the instrument along with the calibration and data processing developed to produce gridded surface elevation maps and snow depth. Section 3 presents an evaluation of the stability and ac-

curacy of the system as well as the spatial resolution. Based on this knowledge of the performance, it then analyses the snow depth time series in terms of physical processes at both sites. Section 4 evaluates the benefit of this instrument compared to single ranging probes in the context of the estimation of the mean snow depth. The present paper focuses on this estimation and does not cover the wide scope of spatial information content of the data set which will be addressed in future work.

2 Materials and method

2.1 Rugged Laser Scan (RLS)

We developed a rugged low-cost laser scan able to operate in harsh conditions like those encountered at Dome C where temperature regularly falls under −70 °C in winter. Despite milder temperature at Col de Porte (a midaltitude French alpine site), rain and occasional storms represent another specific challenge. To minimize the risk, we based this development on an industrial laser meter (DIMETIX FLS-CH 10) which had been used at both sites for several years to carry out point measurements. The performance, robustness and cost were found to be satisfactory. To convert this device designed to take point measurements into a 2-D scanner, we mounted it on a 2-axis stage which performs the rotations in zenith and azimuth as depicted in Fig. 1.

The laser meter has several operating modes to choose from depending on the expected measurement rate and precision. We selected the fast mode, which offers a range accuracy of ±2 mm (statistical confidence level of 95.4 %) at a rate of up to 20 Hz according to the user manual of the device. This rate shall not be confused with the pulse repetition frequency (PRF, Deems et al., 2013), which refers to the number of laser pulses fired in a second. In fact, the PRF is likely much higher than 20 Hz, but is not specified by the constructor in our case. The on-board software is in charge of accumulating and averaging all individual measurements until the estimated accuracy reaches the specifications of the selected mode. For this reason, the effective rate at which the measurements are returned to the user is not fixed and can decrease to under 20 Hz in unfavourable conditions. Among them, it was found during our early tests that the brightness of the environment was an important factor, probably because the photoreceiver becomes saturated or the laser return is weak relative to the background in outdoor conditions. By adding a band-pass optical filter at the laser-operating wavelength (650 nm) on the optical window, we greatly improved the outdoor performances. In addition, collecting the scan at night (or when the sun is at the lowest in Antarctica) also tended to improve the effective measurement rate. The distance and reflectivity of the target are two other important factors controlling the measurement rate. The specifications indicate a maximum range of 65 m when the device is still.

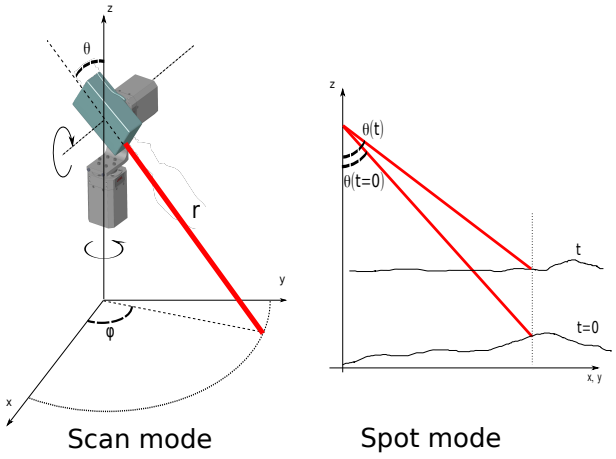

Figure 1. Principle of the scan mode and spot mode of the Rugged Laser Scan (RLS). The zenith angle θ and azimuth angle ϕ determine the orientation of the laser meter which measures the range r.

However, for moving targets – or equivalently when the laser spot moves with respect to the ground as in our application – this range is in practice largely reduced.

In our set-up, the spatial resolution and the time to cover a given surface area depend on both the speed of the spot on the ground and the rate of measurements. With an optimal rate of 20 Hz and a target spatial resolution of 2 cm, it takes nearly 4 h to cover a surface area of 100 m^2. In this case, the spot on the ground moves at $2\,cm \times 20\,Hz = 0.4\,m\,s^{-1}$. Higher speeds have been tried in order to reduce the scan duration but the measurement rate tends to degrade and even abruptly drop for speeds of $0.8\,m\,s^{-1}$ and higher, which completely cancels out any gain.

The scan accuracy (the accuracy of x, y and z) depends on several factors (Deems et al., 2013). The along-range accuracy of the laser meter is 2 mm in ideal conditions, which, projected in terrain coordinates, can be doubled at the maximum zenith angle of 62° used here. In addition, the accuracy depends on the spot size which is about 8 mm in diameter (in the cross range direction) at 10 m and 15 mm at 30 m, according to the manufacturer specifications. Altogether we estimate that the accuracy in z, considering only the laser meter errors and the value given by the manufacturer, could reach 5 mm. Actual performances are presented in Sect. 3.

The 2-axis stage is composed of two identical reduced motors controlled by a feedback on the position. This feedback loop is implemented with an analog proportional–integral–derivative (PID) controller. The accuracy in position is mainly determined by the quality of the potentiometer, which converts the angular position in a resistance, and the electronics, which convert the resistance into a numerical value. The chosen potentiometer model has a linearity of 0.2 % which over a rotation range of 45° corresponds to an accuracy of about 0.1°. A laser scan set up at $z = 4$ m above ground and considering a zenith angle of 62°, this angular er-

ror would translate in 3 cm error on z. It is a significant error for our application, but it is noteworthy that this error is constant in time and should have a limited impact on the snow depth measurements which are obtained by difference. The precision (i.e. the reproducibility in position between different acquisitions) depends on other factors. It is mainly determined by the noise level of the feedback loop and according to our measurements is of the order of 0.03° corresponding to 0.4 cm for a zenith angle of 45° and 1 cm for the maximum angle of 62°. This is 3-fold smaller than the accuracy but is not compensated by differencing. It remains within our target. Note that the analog–digital and digital–analog converters used to measure and command the position have a 16-bit dynamic range and autocalibration, which is largely sufficient given the other above-mentioned sources of error.

2.2 Modes of acquisition

An embedded computer controls the stages and the laser meter. Two different operating configurations have been implemented, called "scan mode" and "spot mode".

In scan mode, the sequence starts by setting the zenith angle θ at its minimum (19.0°). The range is continuously measured by the laser meter while the azimuth stage rotates from $\phi = -90.0°$ to $+90.0°$ at a speed of $v_\phi(\theta)$. The zenith angle is then increased by a small increment $\Delta\theta(\theta)$ and the next arc is completed from $+90.0°$ to $-90.0°$. This process is repeated until the zenith angle reaches the upper limit set to 62°. The speed $v_\phi(\theta)$ and the increment $\Delta\theta(\theta)$ vary as a function of θ in order to ensure a uniform resolution on the surface. Hence, the speed typically ranges from $8\,°\,s^{-1}$ at 20° to $4.2\,°\,s^{-1}$ at 62°. The increment ranges from 0.4 to 0.1°. With such parameters, a scan is completed in 4 h and comprises around 200 000 points. One scan is acquired every day, a balance between scientific relevance and lifetime of the laser meter and mount (the laser itself has a lifetime of 50 000 h at 20 °C according to the manufacturer).

The spot mode was developed to follow the evolution of snow depth with a higher temporal resolution and potentially better accuracy than with the scan mode. This mode monitors a limited set of points which are specified at the beginning of the season by their (x, y) horizontal position. The measurement in spot mode consists of determining the angles (θ, ϕ) so that the laser spot hits the surface of the snow at the vertical of the point (x, y). Figure 1 shows the principle in the vertical plane. The azimuth is constant regardless of the actual snow depth and is easily calculated from x and y. In contrast, the zenith angle depends on the snow surface elevation z, which is unknown and is actually the value we want to measure. An optimization algorithm was implemented to iteratively minimize the horizontal distance between the target point (x, y) and the actual projection of the laser spot in the horizontal plane. This distance is given by $\left|r\sin(\theta) - \sqrt{x^2+y^2}\right|$, where r is the range measured by the laser meter and θ the actual zenith angle. Once this distance is minimized to within a specified tolerance (e.g. 2 cm), 100 measurements of the laser meter and angles are accumulated and averaged with the aim of reducing the reproducibility error. The snow surface elevation z is then calculated with the same formulas as the scan mode. To speed up the optimization process, the optimal angle θ is stored for every point and used as first guess for the next acquisition. In practice, this mode allows us to sample one point in about 30 s, depending on the convergence time of the optimization. We have used this mode at Col de Porte to monitor the snow depth of 64 points in the scanned area over the season every 2 h, except during the 4 h when RLS operates in scan mode (20–24 UTC).

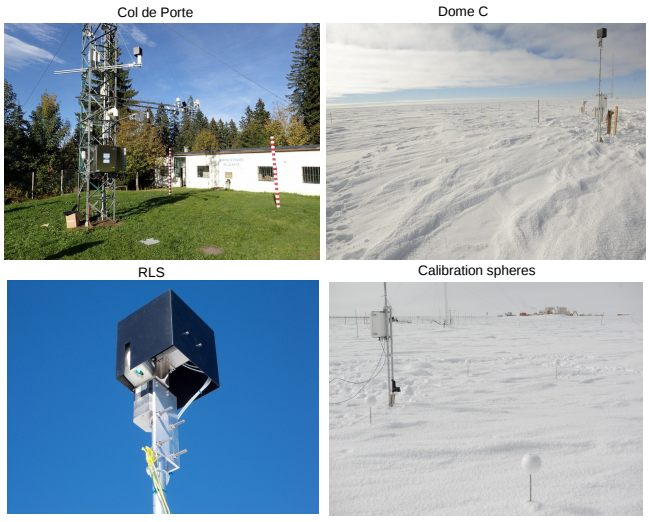

Figure 2. Pictures of RLS during the installation at Col de Porte (October 2014) and at Dome C (December 2014). Zoomed image of RLS (2-axis mount, laser meter and protection) and calibration spheres at Dome C.

2.3 Deployment

Pictures of the set up are shown in Fig. 2. At Col de Porte (left), the laser scan was installed on the meteorological tower of the site at 5.4 m above ground. At Dome C (right), such a big structure would perturb the wind flow and cause artificial accumulation in the scanned area. To limit these effects, we use a very thin structure (38 mm diameter vertical steel rod) and try to avoid wind drag by limiting the installation height to 3.0 m above the surface. The stability of the structure is indeed an important factor for the accuracy (Deems et al., 2015) and can be challenging over a long period. Any movement of the device, either a translation or a rotation, directly results in position errors in the scans. The most likely movement is a tilting of the structure with consequences for both the orientation of the device and its horizontal position. We estimate that stability as small as 0.1°

is required, as it corresponds to about 2 cm bias for an installation height of 5 m. In addition, vertical movements can occur at Dome C because the structure is anchored in the snow. We connected the rod holding the device to a square wood board of 0.3 m^2 buried horizontally at a depth of about 1.5 m. The structure thus sinks as the snow beneath the board densifies. However, this movement is considered negligible compared to the surface elevation variations occurring at the surface due to accumulation, surface snow densification etc. The same approach is used to measure accumulation with stakes (e.g. Magand et al., 2007; Eisen et al., 2008).

To record any movement during the season, we employed two strategies: at Dome C where the snow accumulation is only a few centimetres a year, it was possible to install polystyrene spheres (14.7 cm in diameter) in the field of view of the RLS about 20 cm above the surface. The spheres were mounted on a stick which was anchored into the snow at about 30 cm depth using a small plastic board following the same principle as for the structure. The spherical shape was chosen because the estimation of the centre position from scans can be very robust even with an irregular number of points. Following the (x, y, z) position of the sphere centres allows monitoring of the overall stability of the scanner including the structure, stages and laser meter. Sinking of all the spheres and structure at the same rate would be undetectable but is unlikely. At Col de Porte, spheres were installed at the beginning of the season to check the horizontal levelling of the RLS but they were removed before the first snow because they would be buried during the season and may disturb the accumulation pattern. Instead, we installed a 2-axis inclinometer on the RLS, to record the changes of inclination.

2.4 Data processing

The procedure for computing the position of the points in the (x, y, z) coordinates system from range measurements and stage angles is similar to any TLS and is briefly recalled here with emphasis on some RLS-specific details. It consists of the following steps:

1. The laser meter returns measurements only when a satisfying quality is estimated by the on-board proprietary software, which ensures that the number of unrealistic or inaccurate measurements is limited. Nevertheless, additional checks are needed. A first filter is applied to remove ranges that are too short (< 3 m) and ranges that are too long (> 17 m). A second filter further tracks outliers once the data are projected in (x, y, z) (see below).

2. The position of the spot in the (x, y, z) coordinate system is calculated as follows:

$$z = -r\cos\theta + \Delta_r \sin\theta \quad r_{xy} = r\sin\theta + \Delta_c\cos\theta$$
$$x = r_{xy}\cos\phi \quad y = r_{xy}\sin\phi, \tag{1}$$

   where θ is the zenith angle (laser beam relative to the vertical), ϕ is the azimuth angle and r is the range measured by the laser. Δ_r is the distance between the point $r = 0$ (close to the window of the laser) and the centre of rotation of the laser projected along the beam direction. Δ_c is the same but projected perpendicularly to the beam direction. r_{xy} is the range in the (x,y) plane.

3. Based on an estimate of the levelling of the laser scan (see below), a rotation $\mathcal{R}$ is applied to ensure that the (x, y) plane is perfectly horizontal. In addition, the z coordinate is shifted for convenience so that the origin $z = 0$ is at the mean ground level (for Col de Porte) and on a reference plane (for Dome C) instead of at the centre of rotation of the laser, which is meaningless.

4. The second filter is then applied. It considers that any point higher or lower by 5 cm from the mean height of its neighbours is removed. The neighbourhood is taken as the disk in the horizontal plane of 5 cm in diameter centred at the tested point. This filter is efficient to remove outliers and thin objects like blowing flakes or the cables used to hang the structure. However, it can also erroneously remove areas with a summit or hollow if the local slope is abrupt (over 45°). At last, permanent artefacts in the scanned area (stacks, spheres, etc.) are removed with specific ad hoc criteria.

5. The surface formed by the points (x, y, z) is resampled on a regular grid using the bilinear interpolation implemented in matplotlib.mlab.griddata Python library (version 1.5.1). The same grid is used throughout the season allowing easy calculation of the snow depth and other statistics with weighting. This approach is simple but may degrade the resolution compared to mesh-based approaches (Deems et al., 2013). The chosen spacing was 2 and 3 cm at Col de Porte and Dome C respectively, reflecting the difference of installation height.

The procedure requires a few site-specific inputs, i.e. the rotation matrix and the reference plane. To determine the rotation, we installed four spheres in the scanned area and used a professional laser level to ensure they were in the same horizontal plane with an accuracy estimated to be ± 5 mm. The position of each sphere was determined by first selecting only the points of the scan that reasonably lay in the sphere vicinity based on its expected position (first guess), then minimizing the norm-1 of the function measuring the distance between the points (x, y, z) and the sphere surface: $\sqrt{(x-x_c)^2+(y-y_c)^2+(z-z_c)^2} - R$ where $R = 7.3$ cm is

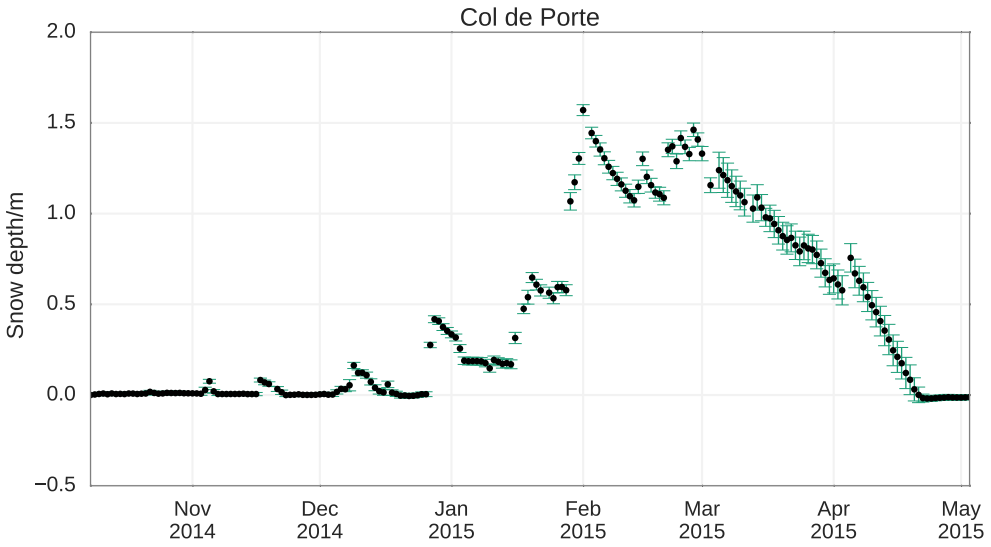

Figure 3. Evolution of the mean (black) and standard deviation (green) of the snow depth at Col de Porte over the winter season 2014–2015 measured by the RLS.

the known sphere radius and (x_c, y_c, z_c) is the unknown sphere centre in the unrotated coordinate system (obtained after step 2). The minimization uses the random sample consensus algorithm (RANSAC, Fischler and Bolles, 1981) to automatically detect and remove outliers. A plane is then fitted onto the four sphere centres by least square fitting and the rotation R which puts this plane horizontal is deduced using the Cloud Compare software. The rotation angle was found to be 0.5° at both Dome C and Col de Porte demonstrating that the levelling of the laser scan mounting was good.

Once rotated, the $z = 0$ reference was taken at the mean elevation of the gridded data for the first scan taken at Dome C (1 January 2015) and for the average of all scans in the snow-free period between 9 and 16 November 2014 at Col de Porte.

2.5 WMO-SPICE data at Col de Porte

For the evaluation of the RLS, we use data collected in the framework of the WMO-SPICE experiment (Rasmussen et al., 2012) at Col de Porte. Two fixed laser meters, OTT/Lufft/Jenoptik SHM 30.11 and Dimetrix FLS-CH 10, were used during the season. They were both set up on the same structure as RLS but shifted by a 2 m-long horizontal arm. The laser meter were tilted by about 20° from the vertical so that the measured footprint was not perturbed by snow accumulating on the arm and sensors and occasionally falling down or melting. However, with such an angle, the footprint position in the horizontal plane moves during the season as a function of the snow depth. It will be shown to be a limitation for the comparison with RLS data. The two snow depth time series were calculated using range measurements, the tilt angles precisely measured for each sensor and the offsets determined using the snow-free period:

$$d_{\text{Dimetix}} = 4.2603 + 0.92666 \times r_{\text{Dimetix}} \quad (2)$$

$$d_{\text{Jenoptik}} = 4.2835 + 0.93643 \times r_{\text{Jenoptik}}. \quad (3)$$

Measurements were carried out every minute during the entire period of operation of the RLS at Col de Porte. For the needs of the WMO-SPICE experiment, the location of these sensors was chosen in an area of the experimental site known to feature generally very low natural variability of snow depth, based on visual inspection over the years. The goal was to concentrate on the possible measurement differences between the instruments tested, which could be due to the instruments themselves.

3 Results

The evolution of snow depth at Col de Porte and of surface elevation (i.e. snow depth with respect to the horizontal reference plane) at Dome C is shown in Figs. 3 and 4. In order to provide an unbiased geophysical interpretation of these variations and distinguish spurious trends from actual variations, which is the ultimate goal of this section, it is necessary to assess in detail the performance, accuracy and precision of the RLS. To this end, we first describe the periods of operation and discuss the causes of failure (Sect. 3.1), then the stability of the instrument and the structure supporting it (Sect. 3.2) and the accuracy in spot and scan mode (Sect. 3.3). The spatial resolution is estimated in Sect. 3.5. Eventually, Sect. 3.6 provides the geophysical interpretation with a knowledge of the limitations.

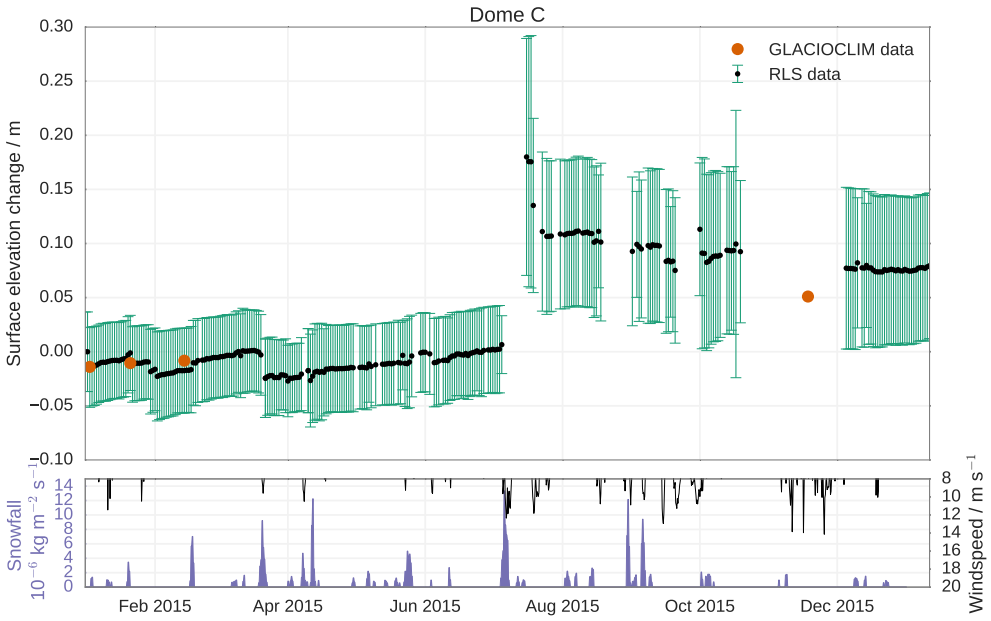

Figure 4. Evolution of the mean (black) and standard deviation (green) of the surface elevation change at Dome C in 2015 and January 2016 measured by the RLS. Orange points show the mean accumulation deduced from emergence measurements of the GLACIOCLIM 50-stack network. The reference is calculated so that the first GLACIOCLIM measurement (3 January 2015) equals the mean RLS snow elevation measured the same day.

3.1 General operating results

The Col de Porte scans were acquired from 7 October 2014 to 3 May 2015 (207 days) with a success rate of 90 %. The snow period started with first ephemeral snowfall on 4 November 2014 and ended on 22 April 2015 when snow was completely absent from the scanned area. At Dome C, the time series ranges between 1 January 2015 and 11 January 2016 when the device was dismantled. A major interruption occurred from 17 October to 5 December 2015 (49 days). Reports of the laser internal temperature indicated malfunction of the internal heating. After a power shutdown from the Concordia station, it started to work again but the stability of the laser temperature was degraded compared to the first period (not shown). Considering that the laser meter has a minimum operating temperature of −40 °C according to the manufacturer and that it was exposed for several months to less than −70 °C, it is possible that the lifetime of the heating element and control electronics were shortened. We cannot, however, conclude that it is the cause of failure based on this single incident. Overall, the success rate over the period is 65 % (and 75 % when excluding the internal heating failure period).

At both sites, the main cause of failure (after the heating failure at Dome C) is the jamming of the stages. This could be caused by snow accumulation in the housing of the device or possibly ice formation on the motors. Since Dome C conditions were windier than Col de Porte and RLS is set up at a lower height than at Col de Porte, the occurrence and impact of blowing snow may be higher, contributing to the lower success rate. In addition, the lower temperature lengthens the recovery time after such an event because of the slower sublimation. The second longest interruption at Dome C from 5 to 16 July following a large accumulation event is very likely to have been caused by this problem. Snow or frost on the laser window is another issue and were the likely cause of a few short interruptions (the laser meter reports the out-of-range error in this case). They were rapidly cleared in 1 or 2 days due to the laser meter heating. Erroneous laser returns due to airborne particles was a minor issue only. The data accumulation and filtering done by the laser meter internal software as well as the filter we implemented removed any occasional short-range acquisitions.

3.2 Stability

3.2.1 Dome C

The stability of the RLS instrument and set-up is evaluated at Dome C using the four spheres installed in an horizontal plane at the beginning of the season. Figure 5 shows the three coordinates of the spheres. Until the event of July 2014, the spheres were detected in nearly every scan. The time series features a few abrupt variations of the order of 3–4 cm and slow trends of up to 1 cm. From July 2015 onwards, the series becomes discontinuous, not only because of the failures of the RLS described in the previous Section, but also because the spheres were entirely (sphere 2) or partially buried (the other three). No other abrupt changes are observed during

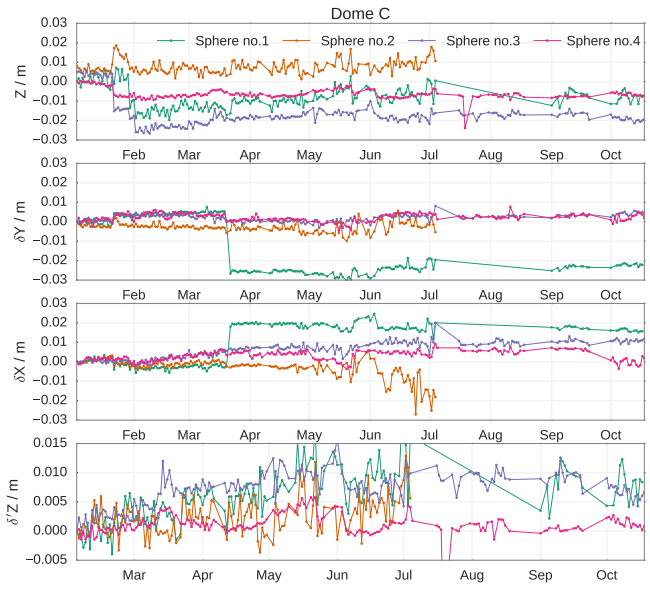

Figure 5. Evolution of the four reference spheres coordinates (x, y, z) at Dome C. δ and δ' respectively refer to the changes with respect to the first scan (1 January 2015) and to a scan just after a period of settling (1 February 2015).

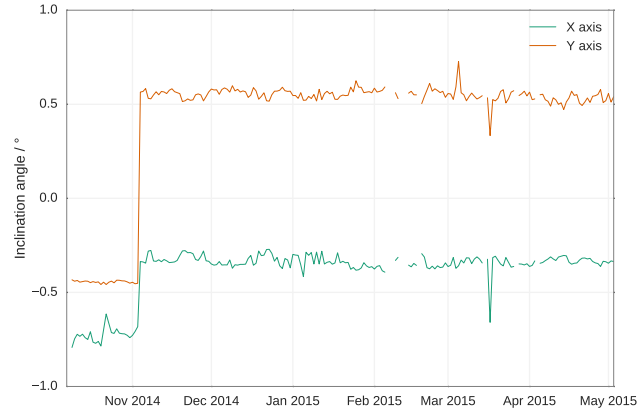

Figure 6. Evolution of the inclination of the laser over the season at Col de Porte.

the second period and the trends seem to remain small, of the order of 1 cm.

In general, the time series depict complex variations which are difficult to understand in term of movements of the structure or the spheres. For instance, the first series of changes in January, visible in z, could be interpreted as a lateral tilting of the structure (two spheres sink while the other two rise), but the absence of significant change in δx and δy at the same time invalidates this hypothesis. Sinking of the spheres due to the densification (the sphere are "anchored" at only 20–30 cm depth) is another possible hypothesis at this time of the year but it fails to explain why the sphere 2 is apparently rising. The sudden and large change experienced by sphere 1 during a wind event in March has the signature of a lateral movement of the sphere itself. At last, slow variations of the elevation $\delta' z$ of spheres 1, 3 and 4 are visible from February to July and seem to reverse from July to January. This could be due to a thermal effect (e.g. dilation of the structure). We also identified periods with hoar forming on the spheres (Champollion et al., 2013), which would result in a positive bias of the z coordinate of the spheres. This highlights the limit of using the spheres as a calibration system.

Nevertheless, despite these uncertainties, the amplitude of the variations give a higher bound of the stability and appear to be acceptable. For the snow depth, the most relevant is the vertical movements of the spheres, which remain within 1 cm over the year if the period of settling after the installation is excluded (January 2015). This is small and acceptable but not negligible compared with the variations depicted in Fig. 4.

3.2.2 Col de Porte

In the absence of spheres, the stability at Col de Porte is evaluated using the 2-axis inclinometer fitted on the laser scan. Figure 6 shows the daily variations along the two axes (calculated by the daily median of the 5 min acquisitions when the scanner is not running). The time series reveals a shift occurring on 3 November 2014 before the first snowfalls. It is most probably due to a maintenance operation on the tower and implies to discard the data before this date, which is not a problem because there are several available snow-free scans after this date.

From 3 November and until the end of the season, the day-to-day variations are of the order of 0.6° on the two axis (specifications of the sensors indicate an accuracy of 0.2° at −10 °C). The long term trend is of the order of a decrease of 0.02° on both axis (too small to be visible in the figure) which is only slightly larger than the long term stability of 0.01° given by the manufacturer. The impact of such a trend on the surface is of the order of 8 mm, in the worst case at 62° zenith angle ($5.2 \times (\tan(62° + 0.02°) - \tan(62°)) = 0.008$). This is acceptable but highlights the need to take precaution on the laser scan mounting as it could be a significant part of the uncertainty budget (Deems et al., 2015).

3.3 Evaluation of the accuracy in spot mode

The comparison between RLS spot mode data and the two fixed laser meters is presented in Fig. 7. The overall variations of snow depth are very similar between the four curves, indicating weak spatial variations between the Dimetix and Jenoptik points (separated by about 1 m) as well as weak differences between the laser meters and RLS. The differences are more apparent on the residual plot in Fig. 7. They range between ±5 cm and vary by 1.0 and 1.8 cm RMS over the season for the Jenoptik and Dimetix points respectively. They show both rapid and slow variations, with an overall negative bias during the accumulation period for both points and

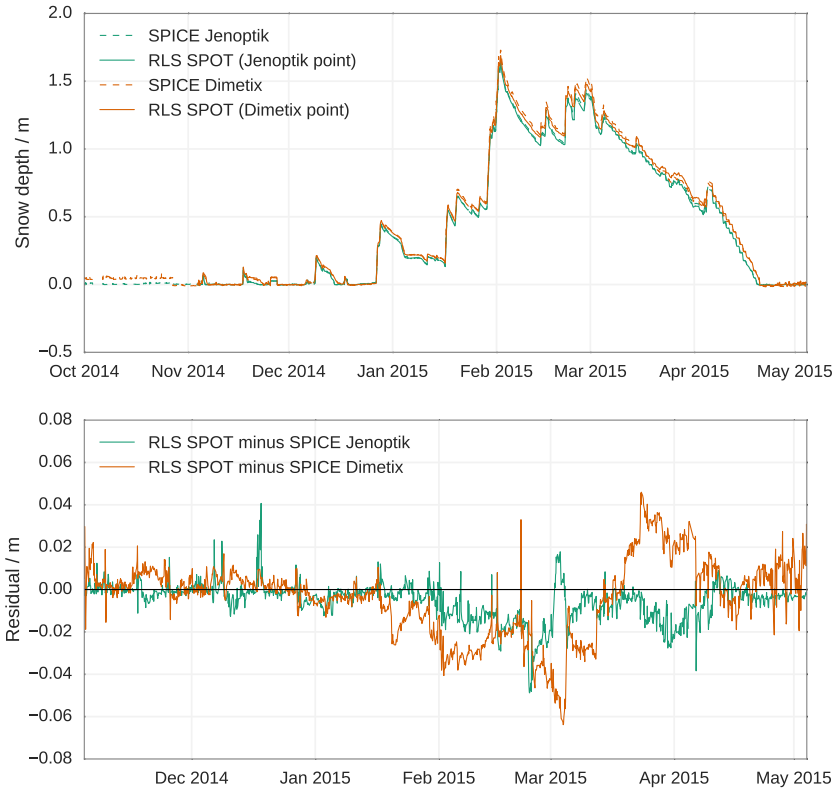

Figure 7. Evaluation of the RLS spot mode against SPICE laser meters at Col de Porte. Top panel shows the depth, bottom panel shows differences between sensors.

a positive bias during the melt period for the Dimetix point only.

Different causes explain these two types of variations. The slow variations seem to be deterministic and could be explained by the slightly different points measured by the sensors. In fact, because of the constant tilt of the fixed sensors, the position of measured point on the surface moves toward the sensors (i.e. to the left in Fig. 8) as the snow depth increases whereas RLS in spot mode measures exactly the same point (x, y) throughout the season. The distance between the measured points when the snow depth is maximum reaches about 60 cm. By looking at the scans we indeed found variations over this distance range of the order of a few centimetres (Fig. 8) with a slope opposite to the sensors which matches the negative bias. Nevertheless, the precise trajectory of the points measured by the laser meters is not known, which prevents any further exploration of this hypothesis.

The rapid variations, on the other hand, are relatively random. This suggests they come from reproducibility errors of the sensors. The weekly standard difference of the 2-hourly data is about 0.4 and 0.7 cm for Jenoptik and Dimetix points on average over the season. The mean daily standard difference is about 0.3 cm for both points. These values are very low and should be compared to the 2σ accuracy of the laser

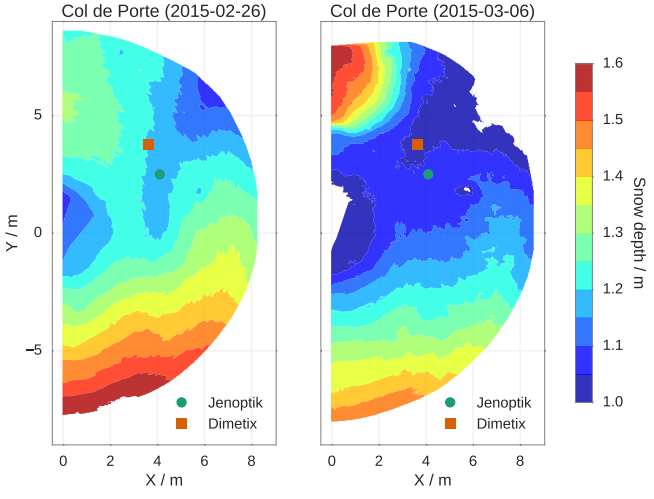

Figure 8. Two snow depth maps acquired at Col de Porte 26 February 2015 when the snow depth reaches its maximum and 6 March 2015 after a wind slab appeared in the northern corner ($x = 0$; $y = 6$ m). North is approximately in the y-axis direction. The square and round symbols represent the footprint of the SPICE sensors at the beginning of the season.

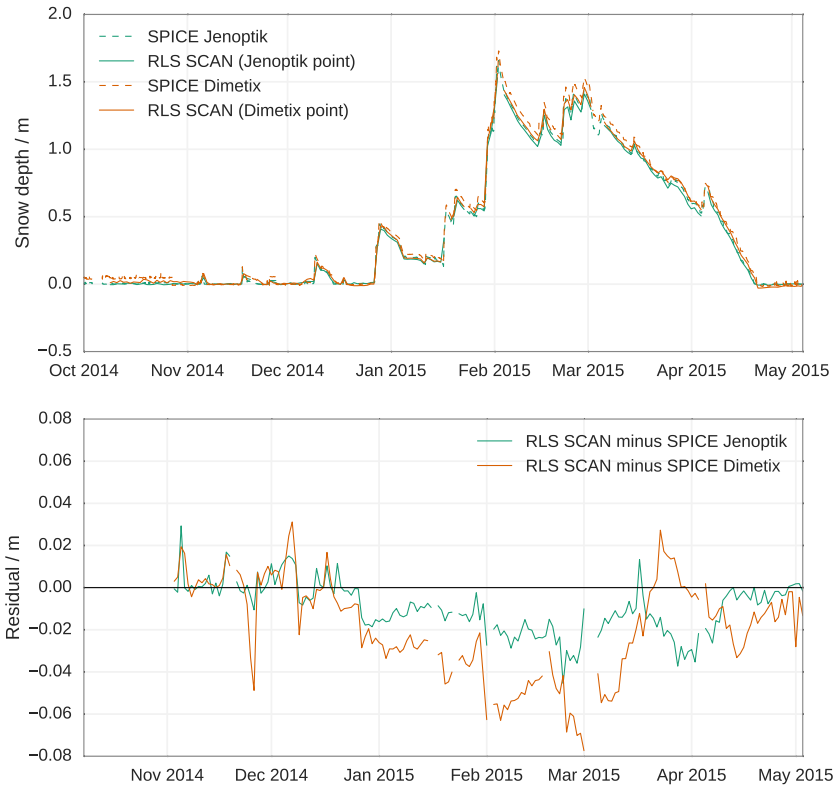

Figure 9. Evaluation of the RLS scan mode against SPICE laser meters.

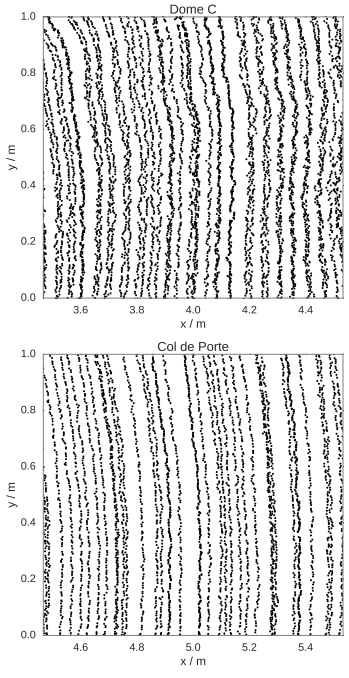

Figure 10. Zoomed image of the scans at Dome C and Col de Porte acquired 15 February 2015. Each point shown in the (x, y) plan is an individual measurement of the laser meter.

meter of about 0.3 cm estimated by the manufacturer. The RLS angle reproducibility error was estimated at 0.03° which is sufficient to explain 0.5 cm RMS (evaluated for a zenith angle of 45° and a laser scan height of 5.2 m).

As a conclusion, we estimate that the spot mode allows a subcentimetre reproducibility for a measurement rate of about 2–3 min^{-1}. With our experimental set-up, we are only able to provide an upper bound on the accuracy of the order of a few centimetres (precise value depends on the metrics, max or RMS differences). A more precise evaluation would require the depth to be compared at exactly the same points over the season. In addition, it would be interesting to use complementary measurement techniques because systematic errors due to the laser meter technique are not taken into account in our evaluation, most notably the penetration depth of the laser in the snow. We expect this error to be small and rather constant of the order of 1 cm (Deems et al., 2013) or lower (Prokop, 2008). As this error does not concern the ground scans, it would tend to negatively bias all the snow depth measurements at Col de Porte, while Dome C would not be affected

3.4 Evaluation of the accuracy in scan mode

To perform the comparison with the fixed sensors data following a similar approach to that of the previous section, we estimated for each scan the z coordinate at constant positions

in the horizontal plane (x, y). We used the same interpolation method as for generating the regularly gridded product (Sect. 2.4) but interpolated at the points monitored in spot mode instead of on the regular grid (the difference would not be more than the grid spacing of 3 cm). In addition, only the fixed sensor data taken simultaneously with the scans (i.e. 20–24 UTC) were considered to avoid differences caused by ongoing snowfalls. The results in Fig. 9 show very similar evolution of the snow depth for the three types of sensors. The daily residual ranges from −8 to +3 cm and is on average 1.2 and 2.3 cm RMS at Jenoptik and Dimetix points, similar to that observed in spot mode. The variations of the residual is also a superposition of rapid variations and a slow component relatively well correlated to the snow depth. The mean weekly standard difference is 0.5 and 0.8 cm at Jenoptik and Dimetix points respectively which is nearly as good as in spot mode. This is unexpected because the latter mode averages a hundred single measurements at the same place, whereas the former is based on interpolation involving four points at most. We conclude that the spot mode unnecessarily oversamples the surface and the number of measurements per point could be reduced, hence allowing for monitoring either more points or more frequently.

Overall this comparison shows that the RLS in scan mode provides similar measurement performances to the fixed sensors or the spot mode even when evaluated at single points. It means that further reduction of the random errors can be obtained by averaging the points over an area.

3.5 Evaluation of the effective spatial resolution

The spatial resolution is an important parameter when not only the mean snow depth but other characteristics of the surface are of interest, such as the distribution of snow depth, roughness, slope, etc. The theoretical spatial resolution can be estimated from scanning parameters (Sect. 2). In the cross-range direction (when the azimuth varies), it is 1.3 cm for the Col de Porte (RLS at 5.2 m height) and 0.7 cm for Dome C (RLS at 3.0 m height). In the range direction, the $\Delta\theta$ increment corresponds to 4.1 cm at the Col de Porte and 2.4 cm at Dome C. Since the increment and azimuth speed are appropriately scaled as a function of the zenith angle during the scan, the theoretical resolution in each direction is constant over the scanned area.

The effective resolution should differ because of the angle reading errors, the laser meter range error and the laser meter measurement rate. It is interesting to evaluate the resolution directly from the scans rather than from the theory. However, this is not straightforward because data are not acquired on a regular grid as highlighted in Fig. 10, which shows the scans of 15 February 2015 at both sites.

The number density of points measurements over the scanned area is about 3100 and 5200 m^{-1} at Col de Porte and Dome C respectively for this date which corresponds to points every 1.8 and 1.4 cm on average if the grid were regular. However, because of the cross-range direction oversampling, these distances are of little interest. The average distance between successive acquisitions (in azimuth) is easy to compute and is 0.9 cm on average at both sites, which gives an estimate of the cross-range resolution. This agrees with the theoretical value considering that the measurement rate can vary around 20 Hz. Combining theses values and number density of points gives a first estimate of the resolution in the other direction. Results are 3.6 cm at Col de Porte and 2.1 m at Dome C which is slightly better than the theoretical value. However, Fig. 10 highlights the irregularity of the zenith increments which we believe to come from the mechanics of the zenith stage and its feedback loop. As a result, the resolution in the zenith direction is irregular and distance between successive zenith increments ranges from 0 cm (i.e. superposition) up to 5 cm at Dome C and 7 cm at Col de Porte in the area covered in Fig. 10. These latter values give an upper limit on the resolution and can be used as conservative estimates.

3.6 Analysis of the evolutions of snow depth and accumulation

To illustrate the capability of the instrument to address geophysical issues which current monitoring systems cannot adequately observe, we provide an example of the use of the RLS data to describe time/space variations of near-surface snow elevation changes at both sites.

3.6.1 Col de Porte

The evolution of the snow depth depicted in Fig. 3 is representative of an alpine midaltitude site. It features a period of accumulation with significant snowfall building up a snowpack up to a depth of 1.46 m (Fig. 8). It is followed by an overall decrease due to the accelerated compaction and melt of the snowpack. With such large accumulation values compared to the precision estimated in Sect. 3.4 and the number of points in the scan (over 150 000), the statistical and instrumental relative errors are always small. The variations of the mean snow depth can be attributed with confidence to physical processes. Even the three ephemeral snowfall events that occurred at the beginning of the season with maximum snow depth (observed at 20 UTC) of 8 cm (4 November 2014), 8 cm (17 November 2014) and 16 cm (8 December 2014) are well described. The standard deviation of snow depth over the scanned area (hereinafter σ_s) is of the order of 1.2–1.7 cm for the three events. As it is close to the reproducibility estimated in Sect. 3.4, we can postulate that the true standard deviation of the snow height is probably smaller than 1.2 cm, that is, the snow depth is very homogeneous. The three next snowfall events show a similar behaviour, despite larger accumulation. Over the accumulation period the standard deviation remains inferior to 4 cm until the maximum is reached on 26 February 2015.

A rain-on-snow event occurred on 1 March 2015, marking the beginning of the melt season. Four days later, a wind slab was formed in the northern corner of the scan ($y \approx +6$ m in Fig. 8). This resulted in a sharp increase of the snow depth standard deviation up to 10 cm, which remained high (around 8 cm) until 22 April 2015, only a few days before the scanned area became entirely snow free. Since the wind slab is only partially viewed by the RLS, the interpretation of the standard deviation value is delicate. Indeed, from a statistical point of view, the snow depth field is not stationary over the sampled area, and while statistical estimators can always be computed, they may be oversensitive to the choice of the sampled area and eventually become useless. This also concerns statistical tests and other frameworks that rely on the assumption of stationarity (Trujillo and Lehning, 2015) and may fail more frequently than predicted by theory. While in practice it is desirable to observe the snow depth field at a large scale to ensure the stationarity, it is not always easy to achieve. It was indeed impracticable in our case, not only because of the limited range of the RLS (limited by the laser meter and by the height of installation), but also because of the size of the Col de Porte site. The site is relatively sheltered compared to higher altitude sites and the area selected for the WMO-SPICE experiment was flat and relatively clear of obstacles. Our results regarding the homogeneity during the accumulation period support a posteriori the choice of this particular area to conduct the WMO-SPICE inter-comparison of snow depth sensors. Nevertheless, a few trees, the main building of the site and the fence are about only 10 m from the scanned and WMO-SPICE area, which makes it difficult to reach stationarity of the snow depth scale. Fortunately, the wind slab – probably formed due to the presence of the trees and the fence – did not expand up to the WMO-SPICE sensor footprints.

3.6.2 Dome C

The evolution of the accumulation is radically different at Dome C (Fig. 3) than it is at Col de Porte. The mean accumulation over the season amounts to only 8 cm which is expected. It corresponds to the annual mean at this site (Petit et al., 1982) and is of the same order as the measurements on the GLACIOCLIM stack network (orange points in Fig. 4) averaging to 6.4 cm over a similar period.

More surprisingly, the time series shows that most of the annual accumulation comes from a single deposition event happening between 5 and 17 July 2015, most likely at the beginning of this period, because we believe it to be responsible for the failure of the instrument. ERA-Interim reanalysis data (Dee et al., 2011) confirm this hypothesis.

It is well known that the deposition is mainly driven by wind on the Antarctic Plateau (Groot Zwaaftink et al., 2013; Libois et al., 2014). Both of these studies showed that when modelling the time evolution of snow accumulation, adding new snow to the snowpack at the time of the precipitation event, as commonly done in alpine environments, was found to be generally inadequate on the Antarctic Plateau. Instead, better results are obtained by pooling snow precipitation into a virtual reservoir until some criteria on the wind speed are met. The reservoir is then emptied on the surface, resulting in a single large deposition event. This tends to delay and reduce the number of the deposition events. Our observation is consistent with this approach, showing that more than six significant snowfalls and a dozen of strong wind events (here $> 8\,\mathrm{m\,s^{-1}}$) predicted by ERA-Interim reanalysis (lower panel in Fig. 4) could have caused significant accumulation but did not. Whether this new observation is a rare or common event, or is biased by the relatively limited scanned area, is an open but important question. Only a longer time series of observations could provide further insights.

In addition to this particular event, the series shows other remarkable patterns of variations, particularly visible during the first part of the series. From February to July, the snow elevation shows two periods of slow and regular increase separated by an erosion event occurring ca. 20 March. During each period approximately 2.5 cm accumulated and the erosion event removed 2 cm in 1 or 2 days. Based on the analysis of the stability (Sect. 3.2) and accuracy (Sect. 3.4), we are confident that these values are real. Such periods of slow accumulation have already been suggested by Picard et al. (2012) based on indirect inferences using microwave remote sensing observations. The 12-year-long time series of satellite data even suggests that most of the accumulation in winter is due to this slow process, which is not captured by the ERA reanalysis. This could be explained by clear-sky precipitation (Walden et al., 2003), hoar growth and/or condensation (Champollion et al., 2013). The rapid erosion event is associated with a strong wind in the reanalysis; however it is worth noting that wind speeds over $8\,\mathrm{m\,s^{-1}}$ are present throughout the period of observations but did not result in erosion. The direction of the wind and pre-existing conditions in the near-surface snowpack are probable factors governing the erosion.

The small temporal evolutions are revealed because many points are averaged. The spatial variability in the scanned area is indeed significant and changes over the time series. In absolute values, it is of the same order as in Col de Porte with $\sigma_s = 3.5$ cm RMS in the beginning of the season and $\sigma_s = 7$ cm RMS in the end. However in relative values, it is about 0.5–1 times the mean annual accumulation whereas at Col de Porte it never exceeds 0.05 of the maximum accumulation.

Since the surface shape frequently changes due to redistribution, the annual accumulation measured at any point is highly variable around the mean. It can even be negative at some point, a case called accumulation hiatus (Courville et al., 2007; Das et al., 2013; Libois et al., 2014). Figure 11 shows the distribution of annual accumulation from RLS over the scanned area together with that calculated from the GLACIOCLIM 50-stakes network near Concordia. The in-

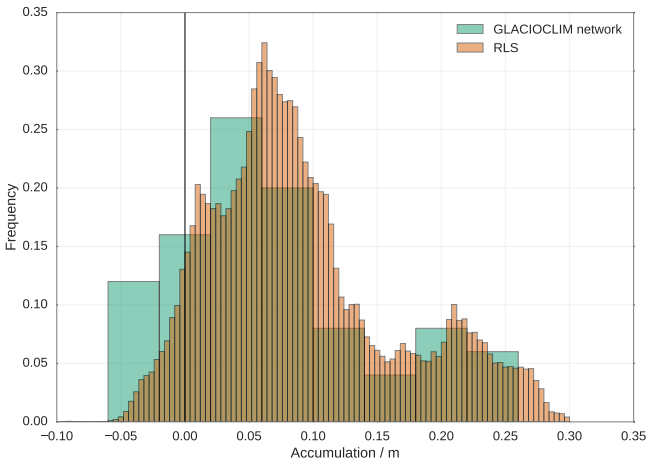

Figure 11. Distribution of the spatial variations of accumulation at Dome C observed by RLS (measured between 3 January and 5 December 2015) and the GLACIOCLIM network at 2 km from Concordia station (measured between 3 January and 18 November 2015).

vestigated periods are slightly different due to the availability of the data but are comparable (3 January 2015 to 18 November 2015 for GLACIOCLIM and to 5 December 2015 for the RLS). The distributions are similar except for a general positive offset for RLS which corresponds to the difference visible on the time series in Fig. 4 between the two spring acquisitions. This similitude is remarkable considering the much smaller area covered by the RLS and the distance between the two sites (about 2 km). It highlights the potential to explore new ranges of spatio-temporal scales using time-lapse laser scanning.

4 Discussions

We have demonstrated that the RLS is able to measure snow depth over a very large number of points with comparable accuracy as with single point sensors. By averaging the spatial variability over these points, the RLS can thus provide mean snow depth over an area of the order of hundreds of square metres with a precision approaching the intrinsic precision of the sensor, i.e. about 1 cm. To evaluate the value of the RLS concept regarding snow depth estimation in a fair way, other factors need to be taken into account. The question is in fact whether a network of N point sensors with an identical overall "cost" could provide the same accuracy or not. The term "cost" here is open and includes different aspects including device price, maintenance, logistical constraints, robustness and risks. This question is closely related to that of designing a snow depth survey from manual measurements (snow course) or equivalently determining the number (and location) of measurements needed to reach some accuracy level. This has been extensively highlighted, e.g. by Grünewald et al. (2013) and investigated in detail by López-Moreno et al. (2011) and Trujillo and Lehning (2015) using geospatial statistical frameworks. However, to apply it in our case is not straightforward because the spatial signal has been shown not to be stationary at both Col de Porte (wind slab) and Dome C (slope). Nevertheless it is possible to obtain similar statistical results by picking random samples from the observed scans which assume ergodicity and negligible spatial correlation. Practically, we consider that N point sensors are randomly located in the scanned area and compare their averaged snow depth to the true snow depth estimated by the average over the whole scanned area. An example for $N = 6$ at Dome C is shown in Fig. 12 along with the independent time series acquired by an ultrasonic ranging probe located about 10 m from the RLS. While the individual trajectories are tangled and each one depicts a particular story about the snow accumulation in 2015, the trends in the 6-point mean looks similar to the scan mean (i.e. true value). Nevertheless it quantitatively differs. The difference gives an estimate of the error ε due to the limited number of observed points. For a large number of random sampling and for different N, we found that the rules $\varepsilon = \sigma_s/\sqrt{N}$ precisely apply despite the non-stationarity and possible correlation. As a result, based on standard deviation σ_s given in Sects. 3.6.1 and 3.6.2, we can estimate that a network of $N = 5$ sensors would have a 1σ error of ≈ 3.5 cm, which is quite large compared to the centimetre precision of the RLS. With $N = 10$, the error is 2.5 cm. To attain an error of 1.5 cm, 30 sensors are necessary. An error of 1 cm requires twice as many sensors. We also should emphasize that these values of error may be over-optimistic as Trujillo and Lehning (2015) found large increases of the standard variation as a function of the size of the covered area, typically 2 to 5-fold between 10 m (the scale of the RLS range) and 100 m because of long-range correlation.

In any case, this demonstrates that a single sensor or a small network is unable to approach the centimetre accuracy and that the spatial variability always dominates the error budget with current sensor technology. While the centimetre accuracy may be inessential for alpine regions, the detection at Dome C of the slow accumulation periods and the zero net accumulation observed during all but one snowfall and strong wind event definitely relies on the ability to average the spatial variability.

Furthermore, the cost of a N-sensor network generally increases with N while the gain in accuracy only follows $\sqrt{N}$. The RLS comes with a higher but fixed cost and provides a large number of points that are sufficient to reduce the error due to the spatial variability to negligible levels. Nevertheless, the current design of RLS provides a limited range which is insufficient to capture some interesting longer spatial scales (Shook and Gray, 1996; Neumann et al., 2006; Picard et al., 2014; Filhol and Sturm, 2015; Trujillo and Lehning, 2015) and could become an issue when long-range spatial correlations are important. While the installation height

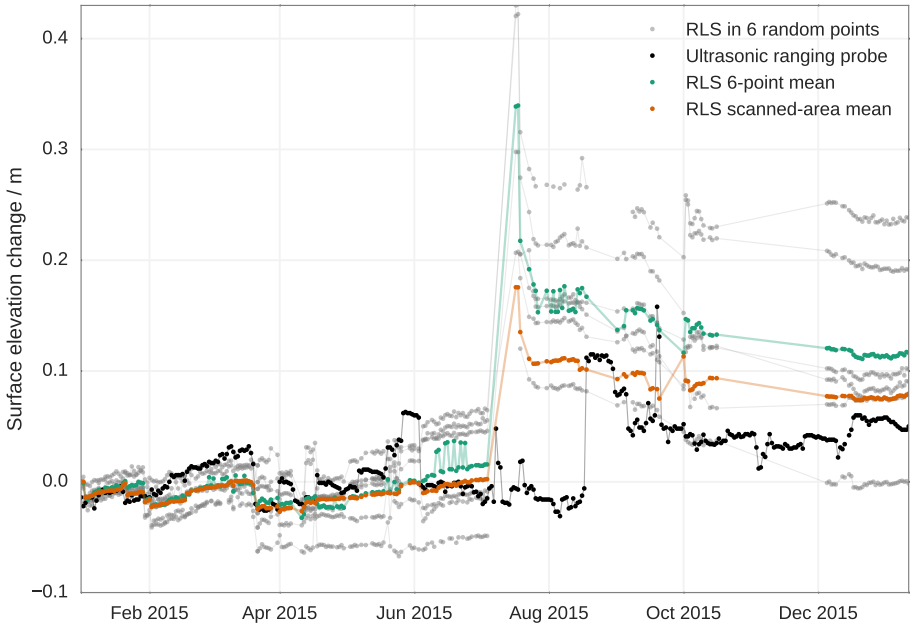

Figure 12. Evolution of the snow surface elevation change at Dome C taken in 6 random points in the scanned area (gray), on average over the 6 points (green), on average over the scanned area (orange) and measured by a nearby ultrasonic ranging probe (black).

could be increased by a few metres to improve this – especially at Dome C where it was only 3 m – some characteristics of the laser meter (maximal range and measurement rate) and the precision of the stages are intrinsically limited. In this domain, the recent commercial laser scans outperform the RLS.

5 Conclusions

This paper shows that a laser meter designed for snow depth point measurements can be transformed into an automatic, robust and low-cost laser scan by adding a 2-axis mechanical stage. About 200 000 points of measurements can be obtained daily, with a precision of the order of 1 cm, and in an area of 150 m^2 when the instrument is set up 5.5 m above the surface. With such a system, the mean snow depth of an area can be estimated with an accuracy approaching the intrinsic accuracy of the instrument, i.e. 1 cm. We estimated that this could not be obtained with a network of point sensors for a similar cost.

The variations of snow depth at Col de Porte over the winter season 2014–2015 is typical of alpine regions, with a few ephemeral snowfalls, then a period of accumulation comprising about six heavy snowfall events, and at last a period of melt. At Dome C, the most remarkable result is that most of the accumulation amount over the year comes from a single event occurring in July. In addition, the time series features periods of slow and regular accumulation without apparent snowfall in the meteorological data, which point to clear-sky precipitation, condensation or hoar formation.

Further work includes improvement of the instrument and further analysis of the data. The rate of failure (mainly due to snow drift) needs to be improved, the power consumption could be optimized in order to make the instrument energy autonomous, and installation at greater heights should be explored to increase the scanned surface area.

This study was focused on the instrument accuracy and the mean snow depth estimation for which the RLS is seen as a provider of numerous independent points of snow depth measurement. However, RLS provides, as any laser scan, maps, that are continuous field of surface elevation and depth whose spatial properties – and spatio-temporal properties for the RLS – are very rich and deserve further exploration. Applications of this new system encompass the study of accumulation process on a broad range of spatial scales and timescales, and the evolution of geometrical and aerodynamical roughnesses for application in remote sensing and surface turbulence.

In the broader context of the WMO-SPICE project, the development of the RLS demonstrates that escaping the limitations of automated point measurements of snow depth due to the spatial variability of the snowpack itself becomes possible only if a significant number (more than 10 typically) of observations are taken simultaneously at the same measurement point (let alone longer range variability, which is particularly significant in mountainous terrain, see e.g. Grünewald et al., 2013). This development paves the way to answer questions and potential operational implementation. In terms of snow depth data assimilation in meteorological or hydrological models, while it is well known that snowpack het-

erogeneity can be found in virtually all environmental contexts, single snow depth values are generally considered representative for given monitoring stations in the assimilation systems, and are most often deducted from a single sensor. Findings by the RLS make it possible to envision the development of future snow monitoring devices which could approach the variability of snow depth at the monitoring station level and, more importantly, determine along with the mean value a quantitative estimate of the spatial variability, which could be considered in the assimilation systems as an indication of the representativeness of the measured mean value. This requires that such measurement campaigns and analyses are repeated in various environmental contexts to assess to what extent the findings in this study apply broadly on all terrestrial land surfaces, and fully assess its implications in terms of the ability to monitor snow depth using single sensors.

Author contributions. Ghislain Picard and Laurent Arnaud developed and built the Rugged Laser Scan (RLS). Jean-Michel Panel managed the laser meters in particular and the Col de Porte infrastructure in general. Samuel Morin coordinated the work in framework of the WMO-SPICE campaign at Col de Porte. All the authors contributed to the evaluation and data analysis and prepared the manuscript.

Acknowledgements. This study was supported by the ANR programme 1-JS56-005-01 MONISNOW and by a grant from OSUG@2020 (investissement d'avenir – ANR10 LABX56). The authors acknowledge the French Polar Institute (IPEV) for the financial and logistic support at Concordia station in Antarctica through the NIVO program. We thank Yves Lejeune, Erwan Le Gac, Jacques Roulle and Laurent Pezard for their help in setting up and running observations at Col de Porte. We thank Eric Lefebvre and Bruno Jourdain for the installation of the laser scan at Dome C and the winter-over staff at Concordia for the maintenance. We thank Vincent Favier and Roxanne Jacob for providing the GLACIOCLIM emergence data. Snow measurements at Col de Porte and Dome C contribute to the SOERE CryObs-Clim observatory and the OSUG CENACLAM observation group. Some of the results presented in this work were obtained as part of the Solid Precipitation Intercomparison Experiment (SPICE) conducted on behalf of the World Meteorological Organization (WMO) Commission for Instruments and Methods of Observation (CIMO). The analysis described herein does not necessarily represent the official outcome of WMO-SPICE. Reference to commercial companies or products is solely for the purposes of information and assessment within the scope of the present work and does not constitute a commercial endorsement of any instrument or instrument manufacturer by the authors or the WMO.

Edited by: Mareile Wolff
Reviewed by: two anonymous referees

References

Cathles, L. M., Abbot, D. S., and MacAyeal, D. R.: Intra-surface radiative transfer limits the geographic extent of snow penitents on horizontal snowfields, Journal of Glaciology, 60, 147–154, doi:10.3189/2014jog13j124, 2014.

Champollion, N., Picard, G., Arnaud, L., Lefebvre, E., and Fily, M.: Hoar crystal development and disappearance at Dome C, Antarctica: observation by near-infrared photography and passive microwave satellite, The Cryosphere, 7, 1247–1262, doi:10.5194/tc-7-1247-2013, 2013.

Clark, M. P., Hendrikx, J., Slater, A. G., Kavetski, D., Anderson, B., Cullen, N. J., Kerr, T., Örn Hreinsson, E., and Woods, R. A.: Representing spatial variability of snow water equivalent in hydrologic and land-surface models: A review, Water Resour. Res., 47, W07539, doi:10.1029/2011wr010745, 2011.

Courville, Z. R., Albert, M. R., Fahnestock, M. A., Cathles IV, L. M., and Shuman, C. A.: Impacts of an accumulation hiatus on the physical properties of firn at a low-accumulation polar site, J. Geophys. Res., 112, F02030, doi:10.1029/2005JF000429, 2007.

Das, I., Bell, R. E., Scambos, T. A., Wolovick, M., Creyts, T. T., Studinger, M., Frearson, N., Nicolas, J. P., Lenaerts, J. T. M., and van den Broeke, M. R.: Influence of persistent wind scour on the surface mass balance of Antarctica, Nat. Geosci., 6, 367–371, doi:10.1038/ngeo1766, 2013.

Dee, D. P., Uppala, S. M., Simmons, A. J., et al.: The ERA-Interim reanalysis: configuration and performance of the data assimilation system, Q. J. Roy. Meteor. Soc., 137, 553–597, doi:10.1002/qj.828, 2011.

Deems, J. S., Painter, T. H., and Finnegan, D. C.: Lidar measurement of snow depth: a review, J. Glaciol., 59, 467–479, doi:10.3189/2013jog12j154, 2013.

Deems, J. S., Gadomski, P. J., Vellone, D., Evanczyk, R., LeWinter, A. L., Birkeland, K. W., and Finnegan, D. C.: Mapping starting zone snow depth with a ground-based lidar to assist avalanche control and forecasting, Cold Reg. Sci. Technol., 120, 197–204, doi:10.1016/j.coldregions.2015.09.002, 2015.

de Rosnay, P., Balsamo, G., Albergel, C., Muñoz-Sabater, J., and Isaksen, L.: Initialisation of Land Surface Variables for Numerical Weather Prediction, Surv. Geophys., 35, 607–621, doi:10.1007/s10712-012-9207-x, 2012.

Eisen, O., Frezzotti, M., Genthon, C., Isaksson, E., Magand, O., van den Broeke, M. R., Dixon, D. A., Ekaykin, A., Holmlund, P., Kameda, T., Karlöf, L., Kaspari, S., Lipenkov, V. Y., Oerter, H., Takahashi, S., and Vaughan, D. G.: Ground-based measurements of spatial and temporal variability of snow accumulation in East Antarctica, Rev. Geophys., 46, RG2001, doi:10.1029/2006rg000218, 2008.

Fierz, C., Armstrong, R. L., Durand, Y., Etchevers, P., Greene, E., McClung, D. M., Nishimura, K., Satyawali, P. K., and Sokratov, S. A.: The international classification for seasonal snow on the ground, IHP-VII Technical Documents in Hydrology No 83, IACS Contribution No 1 UNESCO/IHP, Paris, 2009.

Filhol, S. and Sturm, M.: Snow bedforms: A review, new data, and a formation model, J. Geophys. Res.-Earth, 120, 1645–1669, doi:10.1002/2015jf003529, 2015.

Fischler, M. A. and Bolles, R. C.: Random sample consensus: a paradigm for model fitting with applications to image analysis and automated cartography, Commun. ACM, 24, 381–395, doi:10.1145/358669.358692, 1981.

Genthon, C., Six, D., Scarchilli, C., Ciardini, V., and Frezzotti, M.: Meteorological and snow accumulation gradients across Dome C, East Antarctic plateau, Int. J. Climatol., 36, 455–466, doi:10.1002/joc.4362, 2015.

Gisnås, K., Westermann, S., Schuler, T. V., Melvold, K., and Etzelmüller, B.: Small-scale variation of snow in a regional permafrost model, The Cryosphere, 10, 1201–1215, doi:10.5194/tc-10-1201-2016, 2016.

Groot Zwaaftink, C. D., Cagnati, A., Crepaz, A., Fierz, C., Macelloni, G., Valt, M., and Lehning, M.: Event-driven deposition of snow on the Antarctic Plateau: analyzing field measurements with SNOWPACK, The Cryosphere, 7, 333–347, doi:10.5194/tc-7-333-2013, 2013.

Grünewald, T., Stötter, J., Pomeroy, J. W., Dadic, R., Moreno Baños, I., Marturià, J., Spross, M., Hopkinson, C., Burlando, P., and Lehning, M.: Statistical modelling of the snow depth distribution in open alpine terrain, Hydrol. Earth Syst. Sci., 17, 3005–3021, doi:10.5194/hess-17-3005-2013, 2013.

Hartzell, P. J., Gadomski, P. J., Glennie, C. L., Finnegan, D. C., and Deems, J. S.: Rigorous error propagation for terrestrial laser scanning with application to snow volume uncertainty, J. Glaciol., 61, 1147–1158, doi:10.3189/2015jog15j031, 2015.

Jagt, B., Lucieer, A., Wallace, L., Turner, D., and Durand, M.: Snow Depth Retrieval with UAS Using Photogrammetric Techniques, Geosciences, 5, 264–285, doi:10.3390/geosciences5030264, 2015.

Katlein, C., Arndt, S., Nicolaus, M., Perovich, D. K., Jakuba, M. V., Suman, S., Elliott, S., Whitcomb, L. L., McFarland, C. J., Gerdes, R., Boetius, A., and German, C. R.: Influence of ice thickness and surface properties on light transmission through Arctic sea ice, J. Geophys. Res.-Oceans, 120, 5932–5944, doi:10.1002/2015jc010914, 2015.

Lecomte, O., Fichefet, T., Vancoppenolle, M., and Nicolaus, M.: A new snow thermodynamic scheme for large-scale sea-ice models, Ann. Glaciol., 52, 337–346, doi:10.3189/172756411795931453, 2011.

Libois, Q., Picard, G., Arnaud, L., Morin, S., and Brun, E.: Modeling the impact of snow drift on the decameter-scale variability of snow properties on the Antarctic Plateau, J. Geophys. Res.-Atmos., 119, 11662–11681, doi:10.1002/2014jd022361, 2014.

López-Moreno, J. I., Fassnacht, S. R., Beguería, S., and Latron, J. B. P.: Variability of snow depth at the plot scale: implications for mean depth estimation and sampling strategies, The Cryosphere, 5, 617–629, doi:10.5194/tc-5-617-2011, 2011.

López-Moreno, J. I., Fassnacht, S., Heath, J., Musselman, K., Revuelto, J., Latron, J., Moran-Tejeda, E., and Jonas, T.: Small scale spatial variability of snow density and depth over complex alpine terrain: Implications for estimating snow water equivalent, Adv. Water Resour., 55, 40–52, doi:10.1016/j.advwatres.2012.08.010, 2013.

Magand, O., Genthon, C., Fily, M., Krinner, G., Picard, G., Frezzotti, M., and Ekaykin, A. A.: An up-to-date quality-controlled surface mass balance data set for the 90°–180° Antarctica sector and 1950–2005 period, J. Geophys. Res., 112, D12106, doi:10.1029/2006jd007691, 2007.

Morin, S., Lejeune, Y., Lesaffre, B., Panel, J.-M., Poncet, D., David, P., and Sudul, M.: An 18-yr long (1993–2011) snow and meteorological dataset from a mid-altitude mountain site (Col de Porte, France, 1325 m alt.) for driving and evaluating snowpack models, Earth Syst. Sci. Data, 4, 13–21, doi:10.5194/essd-4-13-2012, 2012.

Mott, R., Schirmer, M., Bavay, M., Grünewald, T., and Lehning, M.: Understanding snow-transport processes shaping the mountain snow-cover, The Cryosphere, 4, 545–559, doi:10.5194/tc-4-545-2010, 2010.

Neumann, N. N., Derksen, C., Smith, C., and Goodison, B.: Characterizing local scale snow cover using point measurements during the winter season, Atmos. Ocean, 44, 257–269, doi:10.3137/ao.440304, 2006.

Nicholson, L. I., Petlicki, M., Partan, B., and MacDonell, S.: 3D surface properties of glacier penitentes over an ablation season, measured using a Microsoft Xbox Kinect, The Cryosphere Discuss., doi:10.5194/tc-2015-207, in review, 2016.

Nolan, M., Larsen, C., and Sturm, M.: Mapping snow depth from manned aircraft on landscape scales at centimeter resolution using structure-from-motion photogrammetry, The Cryosphere, 9, 1445–1463, doi:10.5194/tc-9-1445-2015, 2015.

Petit, J. R., Jouzel, J., Pourchet, M., and Merlivat, L.: A detailed study of snow accumulation and stable isotope content in Dome C (Antarctica), J. Geophys. Res., 87, 4301, doi:10.1029/jc087ic06p04301, 1982.

Picard, G., Domine, F., Krinner, G., Arnaud, L., and Lefebvre, E.: Inhibition of the positive snow-albedo feedback by precipitation in interior Antarctica, Nature Climate Change, 2, 795–798, doi:10.1038/nclimate1590, 2012.

Picard, G., Royer, A., Arnaud, L., and Fily, M.: Influence of meter-scale wind-formed features on the variability of the microwave brightness temperature around Dome C in Antarctica, The Cryosphere, 8, 1105–1119, doi:10.5194/tc-8-1105-2014, 2014.

Prokop, A.: Assessing the applicability of terrestrial laser scanning for spatial snow depth measurements, Cold Reg. Sci. Technol., 54, 155–163, 2008.

Rasmussen, R., Baker, B., Kochendorfer, J., Meyers, T., Landolt, S., Fischer, A. P., Black, J., Thériault, J. M., Kucera, P., Gochis, D., Smith, C., Nitu, R., Hall, M., Ikeda, K., and Gutmann, E.: How Well Are We Measuring Snow: The NOAA/FAA/NCAR Winter Precipitation Test Bed, B. Am. Meteorol. Soc., 93, 811–829, doi:10.1175/bams-d-11-00052.1, 2012.

Revuelto, J., López-Moreno, J. I., Azorin-Molina, C., and Vicente-Serrano, S. M.: Topographic control of snowpack distribution in a small catchment in the central Spanish Pyrenees: intra- and inter-annual persistence, The Cryosphere, 8, 1989=-2006, doi:10.5194/tc-8-1989-2014, 2014.

Revuelto, J., Vionnet, V., Lopez-Moreno, J.-I., Lafaysse, M., and Morin, S.: Combining snowpack modeling and terrestrial laser scanner observations improves the simulation of small scale snow dynamics, J. Hydrol., 533, 291–307, doi:10.1016/j.jhydrol.2015.12.015, 2016.

Ryan, W. A., Doesken, N. J., and Fassnacht, S. R.: Evaluation of Ultrasonic Snow Depth Sensors for U.S. Snow Measurements, J. Atmos. Ocean. Tech., 25, 667–684, doi:10.1175/2007jtecha947.1, 2008.

Schweizer, J.: Snow avalanche formation, Rev. Geophys., 41, 1016, doi:10.1029/2002rg000123, 2003.

Scipión, D. E., Mott, R., Lehning, M., Schneebeli, M., and Berne, A.: Seasonal small-scale spatial variability in alpine snowfall

and snow accumulation, Water Resour. Res., 49, 1446–1457, doi:10.1002/wrcr.20135, 2013.

Shook, K. and Gray, D. M.: Small-scale spatial structure of shallow snowcovers, Hydrol. Process., 10, 1283–1292, doi:10.1002/(sici)1099-1085(199610)10:10<1283::aid-hyp460>3.0.co;2-m, 1996.

Trujillo, E. and Lehning, M.: Theoretical analysis of errors when estimating snow distribution through point measurements, The Cryosphere, 9, 1249–1264, doi:10.5194/tc-9-1249-2015, 2015.

Vionnet, V., Martin, E., Masson, V., Guyomarc'h, G., Naaim-Bouvet, F., Prokop, A., Durand, Y., and Lac, C.: Simulation of wind-induced snow transport and sublimation in alpine terrain using a fully coupled snowpack/atmosphere model, The Cryosphere, 8, 395–415, doi:10.5194/tc-8-395-2014, 2014.

Walden, V. P., Warren, S. G., and Tuttle, E.: Atmospheric Ice Crystals over the Antarctic Plateau in Winter, J. Appl. Meteorol., 42, 1391–1405, doi:10.1175/1520-0450(2003)042<1391:AICOTA>2.0.CO;2, 2003.